Environmental Pollution 289 (2021) 117915

Contents lists available at ScienceDirect

Environmental Pollution

journal homepage: www.elsevier.com/locate/envpol

Budget of riverine nitrogen over the East China Sea shelf

Jing Zhang [a], Xinyu Guo [b,*], Liang Zhao [a]

[a] College of Marine and Environmental Sciences, Tianjin University of Science and Technology, Tianjin, China
[b] Center for Marine Environmental Studies, Ehime University, Matsuyama, Japan

ARTICLE INFO

Keywords:
Nitrogen budget
The Changjiang River
The East China Sea

ABSTRACT

Riverine nitrogen loading to the continental shelf sea is important for terrestrial–marine linkage and global nitrogen cycling and leads to serious marine environmental problems. The budget and cycle of riverine nitrogen over the continental shelf in the East China Sea (ECS) are unknown. Using the tracking technique within a physical–biological coupled model, we quantified the nitrogen budgets of riverine dissolved inorganic nitrogen (DIN) and particulate organic nitrogen (PON) over seasonal to annual scales in the ECS, especially from the Changjiang River, which plays a dominant role in riverine nitrogen input. The horizontal distributions of the Changjiang DIN and PON generally followed the Changjiang diluted water and coastal currents and were affected by stratification in the vertical direction. Their inventory variations were dominated by biological fluxes and modulated by physical ones, and changed most dramatically in the inner shelf among three subregions. Less than half of DIN were converted to PON with most of the rest leaving the ECS through lateral transport pathways, among which the flux through the Tsushima Strait was dominant. With the increasing loading of the Changjiang DIN flux from the 1980s–2010s, lateral transports rather than PON production increased due to limited primary production. Approximately 60 % of the produced PON exported to the sediment and 34 % went to the Tsushima Strait. According to the export production, the DIN from the Changjiang River contributed 12–42 % to the ECS carbon sequestration.

1. Introduction

Continental shelf seas are located between land and open ocean and play an important role in global nitrogen cycling. Large rivers are vital pathways in the terrestrial–marine nitrogen linkage. Riverine loading is a direct nitrogen source for the shelf seas and contributes to the primary production and carbon sequestration there. Because of nitrogen consumption and its biogeochemical cycle in the shelf seas, its outflow flux to the open ocean is not easily estimated from its riverine loading. However, the increase in riverine nutrients has been suggested as a cause of frequent outbreaks of harmful algal blooms, eutrophication, and seasonal hypoxia in the shelf seas (Groβe et al., 2020; Howarth, 2008; Li et al., 2014; Lohrenz et al., 1997). Therefore, constructing riverine nitrogen budgets over the continental shelf is essential for improving our understanding of global nitrogen recycling, demonstrating the land-derived effect on the marine ecosystem and carbon sequestration and solving coastal environmental health problems.

The East China Sea (ECS) is characterized by a broad shelf with complex shelf hydrodynamics and high primary production. As the largest nitrogen input among all the rivers in the ECS, the nitrogen from the Changjiang River is detectable throughout the shelf (Umezawa et al., 2014) and is responsible for environmental issues in coastal and adjacent areas (Gao and Song, 2005; Groβe et al., 2020; Zhang et al., 2007). The nitrogen input from the Changjiang discharge has significantly increased since the 1970s due to rapid urbanization, increased population, intensive industrialization, and large-scale chemical fertilizer use in the Changjiang River Basin (Dai et al., 2011; Liu et al., 2015, 2018; Wang, 2006). It has been reported that the increased nutrients from the Changjiang River, especially the dissolved inorganic nitrogen (DIN), have caused the rapid increase in the frequency and area of harmful algal blooms (Li et al., 2014), as well as impacted the seafloor oxygen demand and the intensified coastal bottom hypoxia area (Liu et al., 2015). Therefore, it is of great significance to clarify the riverine nitrogen budget and further evaluate its physical and biological processes in the Changjiang Estuary and adjacent shelf areas.

Changjiang River diluted water (CDW) is the main factor impacting the shallow estuary and adjacent areas, and it influences the northern areas in June and the southern areas in November (Wang et al., 2017).

* Corresponding author. Center for Marine Environmental Studies, Ehime University, 2-5 Bunkyo-Cho, Matsuyama, 790-8577, Japan.
E-mail address: guoxinyu@sci.ehime-u.ac.jp (X. Guo).

https://doi.org/10.1016/j.envpol.2021.117915
Received 26 January 2021; Received in revised form 14 July 2021; Accepted 4 August 2021
Available online 6 August 2021

Accordingly, the nutrients from the Changjiang River are largely restricted to the estuary, while the ecosystem outside the estuary is mainly supported by other nutrient sources (Liu et al., 2009). However, people also argue that the nutrients from the Changjiang River can be transported a long distance offshore, because they are not consumed effectively by phytoplankton in the estuary due to the high turbidity (Isobe and Matsuno, 2008), which eventually affects the Tsushima Strait in summer (Isobe et al., 2002; Morimoto et al., 2012) and results in autumn blooms in the broader regions of the Japan Sea (Shibano et al., 2019).

Although riverine dissolved nitrogen content has been studied, its extent and transport mechanisms from the Changjiang River to the open ocean and its fate within the shelf area remains unclear. The transport and budget of particulate nitrogen produced by the riverine dissolved nitrogen over the ECS shelf are also unclear although they are needed for completing the overall understanding of nitrogen cycling and dynamics (Yu et al., 2012; Zuo et al., 2016). Consequently, we cannot even answer the essential problem of how much and in which form the riverine nitrogen is exported to sediment and to the open ocean.

The nitrogen budget in the ECS has been estimated based on field observations and numerical models (e.g., Liu et al., 2020; Wang et al., 2019; Zhang et al., 2007), but few studies have focused on the cycling and budget of riverine nitrogen. Stable isotope measurements can distinguish riverine nitrogen (Umezawa et al., 2014; Yan et al., 2017; Zhong et al., 2020), although the strong spatial and temporal variations in the marine environment and nitrogen cycle increases the uncertainty of those estimations. Using biogeochemical coupled models can provide a precise nitrogen budget (Estrada-Allis et al., 2020; Fennel et al., 2006; Wang et al., 2019; Xue et al., 2013; Zhang et al., 2019b) by considering the nitrogen from all sources rather than a single riverine one. The technique of tracing nitrogen from an external source in a simulated ecosystem is an effective way to interrogate the problem (Kawamiya, 2001; Ménesguen et al., 2006) as it can track nutrients from a specific source and consider both physical and biological processes. Therefore, we provide such an analysis here.

In this study, we investigate transport and budget of riverine dissolved nitrogen and its produced particulate nitrogen in the ECS using a physical–biological coupled model with a tracking module. Furthermore, we interpret the riverine nitrogen budget response over the ECS according to the change in riverine nitrogen input. Finally, we evaluate the role of riverine nitrogen in export production and carbon sequestration.

2. Method

The model covers the region from 24.0 to 41.0° N and from 117.5 to 131.5° E with a resolution of 1/18° (5–6 km) and 21 σ layers (Fig. 1). The 50-m, 100-m, and 200-m isobaths along with the Taiwan Strait section (TAS), 34.7° N section (34N), and the Tsushima Strait section (TUS) separate the ECS into three subregions: the inner (0–50 m), middle (50–100 m), and outer shelves (100–200 m), which are used in the nitrogen budget evaluation.

The model consists of two parts. The first part is a physical–biological coupled model based on Zhao and Guo (2011) and Wang et al. (2019), which is used for calculating the cycles of all nitrogen sources. Biogeochemical processes in the water column in this model include photosynthesis, respiration, and mortality of phytoplankton, and remineralization of detritus, while those in the benthic layer include remineralization and denitrification. Wang et al. (2019) analyzed the nitrogen budget from all ECS sources based on the results from the same physical–biological coupled model.

The second part is the tracking model following the method in Ménesguen et al. (2006), which separately calculates the state variables from different nitrogen sources. We applied it here to calculate the nitrogen budget from riverine source. The method in this study is the same as that used in Zhang et al. (2019a), but only the DIN tracking case was applied here and the target sources were changed to many rivers.

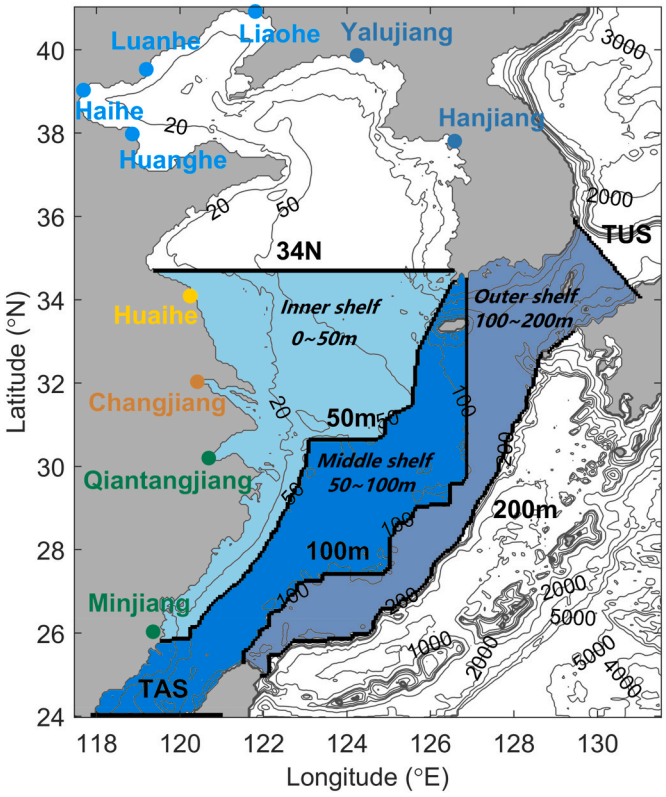

Fig. 1. The model domain and bathymetry. The grey contour lines represent the isobaths. The dots along the coast denote the positions of inflow from rivers and the same group of rivers has the same color. The black thick line shows the positions of the Taiwan Strait (TAS), Tsushima Strait (TUS), 34.7° N section (34N), and three designated isobaths sections: 50-m, 100-m, and 200-m isobaths. Note that the Cheju Strait section is appended to the 100-m isobath for convenience. With these sections, the ECS is divided into the inner shelf (0–50 m), middle shelf (50–100 m), and outer shelf (100–200 m) subregions. (For interpretation of the references to color in this figure legend, the reader is referred to the Web version of this article.)

There are ten main rivers loading nutrients into the ECS in our study area. We divided them into five groups according to location: (1) the Changjiang (Yangtze River), (2) the Minjiang and Qiantangjiang rivers in the southern ECS, (3) the Huanghe, Haihe, Luanhe, and Liaohe rivers emptying into the Bohai Sea, (4) the Huaihe River in the southern Yellow Sea, and (5) the Yalujiang and Hanjiang rivers in the northern Yellow Sea. The nitrogen-related state variables, namely DIN, phytoplankton, and detritus, with a label of five groups were tracked in the model.

Notably, even though only the nitrogen from five river groups was tracked, the physical–biological model considered the input of all external nutrient sources, including atmospheric deposition and those from Taiwan Strait and Kuroshio. The biogeochemical processes in the model are calculated based on the total nutrient concentration, and then separated to each source of DIN based on the ratio of one specific DIN concentration to total DIN concentration. The tracking module is applied to separate the riverine dissolved and particulate nitrogen fraction.

In our default calculation, we set the concentrations of DIN, dissolved inorganic phosphorus (DIP), and silicate in the Changjiang River to the 2010 levels, which are 110.2, 1.39, and 107.6 mmol m^{-3}, respectively (Liang and Xian, 2018). The nutrient concentrations from other rivers were taken from published data (Liu et al., 2009; Zhang, 1996). At the beginning of the tracking module, the riverine DIN was pumped into the ECS through the estuaries where its related state

variables have a value of zero. Then phytoplankton and detritus supported by the riverine DIN are generated over the continental shelf. Their sum is defined as particulate organic nitrogen (PON) here. It is noted that the model does not consider the input flux of dissolved organic nitrogen (DON) and PON from rivers because they only comprise 18 % and 7 % of the total Changjiang River nitrogen input flux (Kwon et al., 2018; Zhang et al., 2003).

Under the circumstances, the riverine DIN-tracking case was run for over 5 years until the state variables reached a stationary state and the results in the final calculation year are used for our analysis. The annual mean fluxes of DIN directly pumped into the study area from the Changjiang River (Group 1), Minjiang and Qiantangjiang rivers (Group 2), and Huaihe River (Group 4) are 3.22, 0.22, and 0.05 kmol s^{-1}, respectively. The model results for the DIN from the Changjiang River are mainly presented in the following sections because its input flux occupies 92 % (3.22/3.49) of all the riverine DIN sources. The DIN from the Changjiang River and its supported PON are denoted by DIN_C and PON_C.

The physical–biological coupled model without the tracking module has been approved to be able to reproduce the general circulation and the spatial-temporal variations in biological variables in the ECS (Wang et al., 2019; Zhang et al., 2019a; Zhao and Guo, 2011). Both the spatial-temporal variations of DIN and PON agree well with observations (Figs. 2–8 in Wang et al., 2019, Fig. 4 in Zhang et al., 2019a), and the DIN fluxes from external sources are comparable to previous studies (Table 4 in Wang et al., 2019). These factors are critical for the reliability of the tracking module.

3. Results and discussion

3.1. Horizontal distributions of DIN_C and PON_C

The surface distributions of DIN_C concentration are shown in Fig. 2a–d. The DIN_C concentration was extremely high in the inner shelf in winter, more than 50 mmol m^{-3}. The DIN_C headed southward following the Min-Zhe Coastal Current south of the Changjiang Estuary (Chen, 2008; Wu et al., 2013). In the spring, the DIN_C north of the Changjiang Estuary expanded to the northeast while the DIN_C south of the estuary decreased. The CDW brought the DIN_C to the Tsushima Strait in the summer (Chang and Isobe, 2003; Isobe and Matsuno, 2008). Unlike DIP, the DIN_C could not be fully assimilated locally and was transported to the Tsushima Strait (Zhang et al., 2019a). Meanwhile, the DIN_C concentration from the southern coast further decreased. In autumn, the northeastward DIN_C retreated and turned southward along the coast (Bi et al., 2018). In general, the surface DIN_C seasonal patterns followed the CDW and coastal current distributions.

In winter and autumn, the patterns of DIN_C in the bottom layer were similar to those in the surface layer due to the strong vertical mixing (Fig. 2e, h). The concentration DIN_C in the bottom layer in spring was relatively lower than that in the surface layer (Fig. 2f). The largest difference between the DIN_C concentration in surface and bottom layers occurred in summer when stratification became strongest (Li et al., 2006; Quan et al., 2013). The bottom DIN_C concentration was relatively high in the Cheju Strait in summer and autumn. The extension of Changjiang Diluted Water transported high-concentration unexhausted DIN_C nearshore to the Cheju Strait.

PON_C generally had a lower concentration than DIN_C (Fig. 3). The seasonal variation in the PON_C in the surface layer was weak, with a high concentration region lying in the same inner shelf. The surface PON_C in summer was mainly confined to the coastal area rather than heading to the Tsushima Strait like the DIN_C. The PON_C concentration was higher in the bottom layer than in the surface layer and showed a slightly strong seasonal variation with a maximum value appearing in summer. Like DIN_C, the PON_C concentration in the bottom and surface layers showed the greatest difference in summer.

3.2. Seasonal variations in DIN_C and PON_C fluxes

The inventories of DIN_C and PON_C over a region are controlled by both physical and biological processes in the model (Wang et al., 2019). The DIN_C and PON_C are related through biological processes including photosynthesis, respiration, and remineralization. A negative value of all these biological fluxes of PON_C indicates that their net effect is a transformation of PON_C to DIN_C. Naturally, their biological fluxes showed an opposite variation. The physical processes for DIN_C and PON_C consist of river loading (only for DIN_C), water–sediment flux at the sea bottom, and horizontal fluxes through the lateral boundaries of the region. The water–sediment flux for DIN_C resulted from the regenerated DIN from sediments, and that for PON_C was a sum of sinking and resuspension of PON. Time variation terms in DIN_C and PON_C inventories are shown in Fig. 4, with the aforementioned physical and biological fluxes. The positive (negative) value of flux induces the increase (decrease) in inventory. The seasonal variations in DIN_C and PON_C fluxes and the connections among the three subregions are given below.

The DIN flux loading from the Changjiang River (*Riv*) peaked in summer as a result of large river discharges in the rainy season (Fig. 4a). Among all the fluxes in the inner shelf (Fig. 4a), *Riv* was the largest with an annual value of 3.22 kmol s^{-1} (= 142.3 × 10^4 t yr^{-1}), which was comparable to observed values (135.3 × 10^4 t yr^{-1}, Guo et al., 2015). The seasonal variation in DIN_C water–sediment flux (*Bot*) was weak, and a slightly higher value appeared in September corresponding to the large *Bot* PON_C flux. The biological flux (*Bio*) of DIN_C was the largest negative flux in the inner shelf with an annual average of 1.27 kmol s^{-1}. Here, the negative value denotes a DIN_C sink. The consumption of DIN_C dominated all the biological processes from March to November while

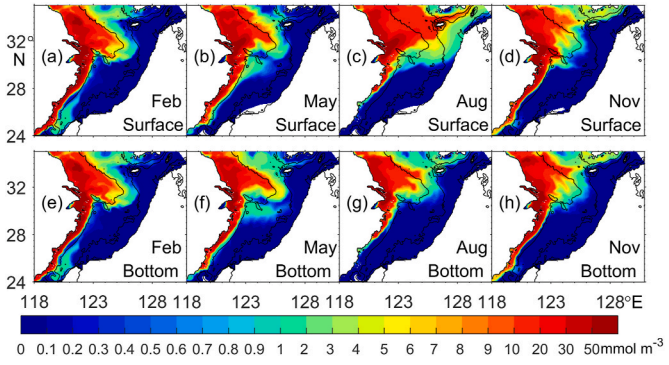

Fig. 2. Seasonal distributions of DIN concentration from the Changjiang River (DIN_C) at the (a–d) surface layer and (e–h) bottom layer (unit: mmol m^{-3}). The concentration outside the shelf area is not shown.

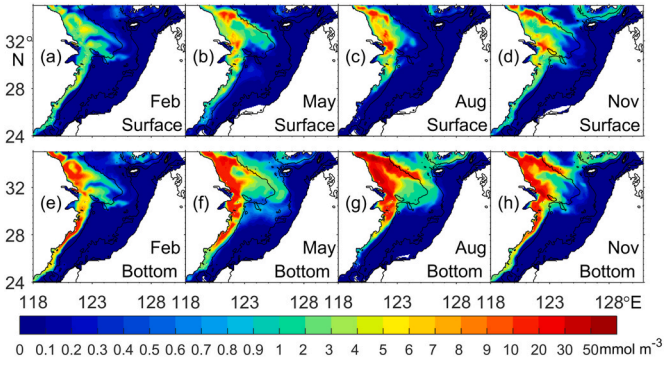

Fig. 3. Seasonal distributions of PON concentration from the Changjiang River (PON_C) at the (a–d) surface layer and (e–h) bottom layer (unit: mmol m^{-3}). The concentration outside the shelf area is not shown.

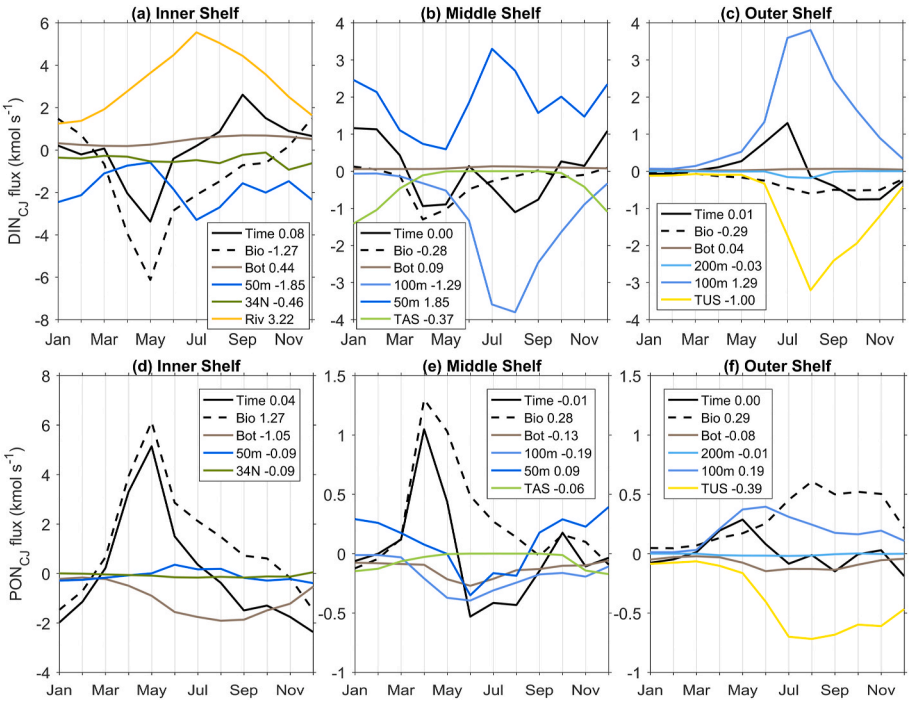

Fig. 4. The inventory-related fluxes of (a–c) DIN_C and (d–f) PON_C over the inner, middle, and outer shelves of the ECS. The time variation term of the DIN_C or PON_C inventory is denoted by *Time*. The biological flux is denoted by *Bio*. The flux across the water–sediment interface is denoted by *Bot*. The fluxes across lateral sections are indicated by *200m, 100m, 50m, TUS, TAS,* and *34N* (see Fig. 1 for the position of each section). The values in the legend are annual means of the corresponding fluxes. The positive (negative) value of flux induces the increase (decrease) in inventory.

regeneration occurred in the remaining time. The other large negative flux of DIN_C in the inner shelf was through lateral transport across the 50-m isobath section, which had two peak times, one in July due to the CDW, and the other in winter due to southward coastal currents. The remaining few fluxes of DIN_C in the inner shelf headed to the Yellow Sea through the 34N section. Overall, the inventory of DIN_C in the inner shelf decreased from March to June because of *Bio* flux and then increased with *Riv* loading.

One difference of the DIN_C *Time* term in the middle shelf from that in the inner shelf was an extra negative peak in summer (Fig. 4b), resulting from the largest output flux across the 100-m isobath section due to the large across-isobath volume transport there (Zhang et al., 2017). Another exit for the DIN_C in the middle shelf was the Taiwan Strait (*TAS*); however, this route was only possible in winter because of the strong northeasterly winds (Oey et al., 2014). The *Bio* flux in the middle shelf shared a similar seasonal variation with that in the inner shelf although its magnitude was smaller than the two across-isobath fluxes (50-m and 100-m). The increase in the DIN_C in the middle shelf was attributed to the lateral flux across the 50-m isobath from the inner shelf as the other positive flux was the release of DIN from the sediment, which was substantially smaller than that in the inner shelf.

The tendency of DIN_C in the outer shelf (Fig. 4c) was unlike that in the inner and middle shelves (Fig. 4a and b). The DIN_C increased in spring and summer but decreased in autumn and winter, indicating the small effect of the biological fluxes. All the fluxes were weak in winter. As the temperature rose, the biological consumption of DIN_C increased and reached the maximum in summer rather than in spring. The fluxes across the 100-m isobath and through the Tsushima Strait (*TUS*) were comparable and shared similar seasonal patterns, peaking in August. Only a small portion of DIN_C left the shelf across the 200-m isobath.

The PON_C fluxes are shown in the lower panel in Fig. 4. In contrast to the DIN_C, the biological processes increased the PON_C rapidly over the inner shelf in spring (Fig. 4d). Subsequently, the loss of PON_C to the sediment (the combined effect of sinking and resuspension) was strongest in August and September, and was the main export pathway of PON_C in the inner shelf. The lateral fluxes of PON_C were significantly smaller than the water–sediment and biological fluxes. The PON_C flux across the 50-m isobath showed a positive value in summer, rather than a CDW-related negative value. Previous study has shown that the volume transport across the 50-m isobath in summer was in the onshore direction in the bottom layer (Zhang et al., 2017) where the concentration of PON_C was higher than that in the surface layer (Fig. 3g).

The *Bio* flux was still the largest one among the PON_C fluxes in the middle shelf (Fig. 4e). The strongest offshore PON_C flux across the 100-m isobath section followed the *Bio* peak and occurred in June, two months earlier than the DIN_C lateral flux through the same section. Different peak times of PON_C and DIN_C fluxes are caused by their different concentrations. The PON_C in the middle shelf are produced in the largest quantities in April, which contributes to its increasing offshore transport across 100-m isobath to outer shelf in May and June. When it comes to summer (e.g. August), the DIN_C fluxes across 50-m isobath from the inner to the middle shelf peaks following the Changjiang input and the consumption of DIN_C in the middle shelf weakens. Their combined effect results in the highest fluxes of DIN_C across 100-m isobaths in August.

The time variation term of PON_C in the outer shelf was similar to that of DIN_C (Fig. 4f), but peaked in May, also two months earlier than the DIN_C. The fluxes of PON_C and DIN_C across 100-m isobath contribute most to these two peaks. The positive fluxes, inflow across 100-m isobath, and biological flux, were primarily balanced by the flux through the Tsushima Strait.

The time variation in DIN_C over the whole shelf followed the pattern in the inner shelf because the biological and physical fluxes of DIN_C there were largest, as did the PON_C. The time variations of inventories of DIN_C and PON_C were affected by both biological and physical processes.

3.3. Annual budgets of DIN_C and PON_C

Fig. 5 shows the DIN_C and PON_C budgets for the ECS continental shelf. The sum of DIN_C and PON_C is referred to as total nitrogen (TN_C) here. The nitrogen budget is given in the three subregions. In the inner shelf, the DIN_C sources are the Changjiang River input (3.22 kmol s^{-1}) and the bottom sediment release (0.44 kmol s^{-1}). Approximately 35 % of the DIN_C input is converted to PON_C through biological processes (1.27 kmol s^{-1}). Most unexploited DIN_C leaves the inner shelf to the Yellow Sea via the 34N section and to the middle shelf across the 50-m

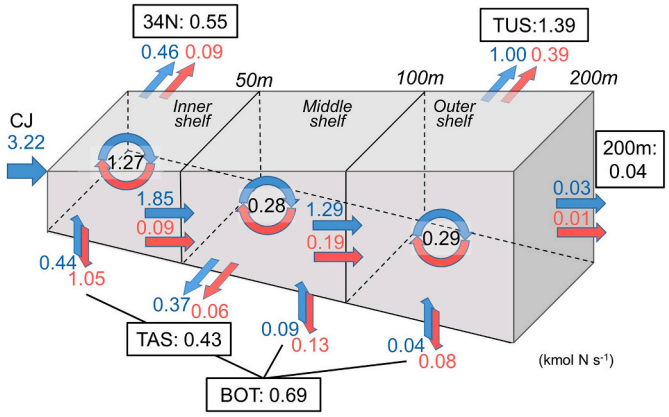

Fig. 5. Annual budgets of DIN_C and PON_C over the inner, middle, and outer shelves of the ECS. The straight blue (red) arrows with numbers denote the annual mean flux of DIN_C (PON_C). The value in each black box denotes the flux of total nitrogen (TN_C). The values inside the three circles denote the transformation flux between DIN_C and PON_C. All values are in kmol N s^{-1}. (For interpretation of the references to color in this figure legend, the reader is referred to the Web version of this article.)

isobath section, which accounts for over 50 % of the DIN_C input (1.85 kmol s^{-1}). The PON_C fluxes into the Yellow Sea and the middle shelf are small and comprise only 14 % (= 0.18/1.27) of the generated PON_C. Most PON_C (83 %) is deposited on the sea bottom with an annual mean flux of 1.05 kmol s^{-1}; meanwhile, the DIN_C returns to the water column with a flux of 0.44 kmol s^{-1}. Consequently, the TN_C is lost to the sediment with a flux of 0.61 (1.05–0.44) kmol s^{-1}, which is the largest value among the three subregions. The TN_C budget in the inner shelf shows an input flux of 3.22 kmol s^{-1} from the Changjiang River and a total of 3.10 kmol s^{-1} of output flux that consists of 0.55 kmol s^{-1} (0.46 DIN_C+0.09 PON_C) through 34N, 1.94 kmol s^{-1} (1.85 DIN_C +0.09 PON_C) across the 50-m isobath and 0.61 kmol s^{-1} (1.05 PON_C -0.44 DIN_C) across the water-sediment interface. The difference between the input flux and total output flux is 0.12 kmol s^{-1}, which equals to the sum of the time-variation terms of DIN_C (0.08 kmol s^{-1}) and PON_C (0.04 kmol s^{-1}) in the inner shelf.

The middle shelf receives TN_C from the inner shelf across the 50-m isobath section, of which DIN_C and PON_C account for 95 % (1.85 kmol s^{-1}) and 5 % (0.09 kmol s^{-1}), respectively. Adding the bottom DIN_C flux (0.09 kmol s^{-1}), the input flux of DIN_C reaches 1.94 kmol s^{-1} in the middle shelf. The generated rate of PON_C (0.28 kmol s^{-1}) represents 14 % of the input flux of DIN_C, lower than the transformation efficiency in the inner shelf (35 %). The ratio (46 % = 0.13/0.28) of PON_C water–sediment flux to the generated PON_C in the water column is also less than that in the inner shelf (83 %) due to greater water depth. The aphotic layer is thicker in the middle shelf than in the inner shelf. With a constant sinking rate, the detritus has more time to decompose in the middle shelf than in the inner shelf before reaching the sea bottom. Consequently, fewer PON_C reaches the sea bottom of the middle shelf than that of the inner shelf. The TN_C in the middle shelf exports to the outer shelf across the 100-m isobath section, to the South China Sea across the *TAS* section and to the sea bottom through water–sediment interface. The sea bottom has the lowest export flux with an average of 0.04 kmol s^{-1} (0.13–0.09), while the former two are more important. The ratios of PON_C to TN_C in lateral transport increase from 5 % at the 50-m isobath section to 13–14 % at the 100-m isobath and *TAS* sections.

The inflow of DIN_C (1.33 kmol s^{-1}) in the outer shelf comes from the middle shelf (1.29 kmol s^{-1}) and the bottom sediment (0.04 kmol s^{-1}), 22 % of which is converted to PON_C. The generated PON_C with the inflow from the middle shelf (0.19 kmol s^{-1}) contributes to 0.48 kmol s^{-1} input flux of PON_C in the outer shelf. Only one-sixth of input PON_C is exported to the bottom sediment (0.08 kmol s^{-1}), indicating the important role of export through lateral transport. The PON_C contributes 25 % and 28 % of TN_C fluxes across 200-m isobath and the *TUS* section, respectively. The outflow of DIN_C through the *TUS* section (1.00 kmol s^{-1}) is two orders of magnitude larger than that across the 200-m isobath section (0.03 kmol s^{-1}).

In general, lateral DIN_C transport plays a more active role in the DIN_C budget. Only a small proportion of DIN_C transforms to PON_C over three subregions, among which the amount and conversion efficiency are largest in the inner shelf. The water–sediment flux of PON_C also peaks in the inner shelf and sharply decreases in the middle and outer shelves. By contrast, the lateral transports of PON_C in the middle and outer shelves increase.

In this estimation, the nitrogen budgets from the five groups show different patterns according to their different locations (Table .1). The input from the Changjiang River is the only source of DIN while its transformation to PON_C and lateral fluxes are the sinks. The lateral fluxes of DIN_C are an essential way of acting as a sink, especially through the Tsushima Strait. Large amounts of produced PON_C export to the seabed, while some go to the Tsushima Strait. The Minjiang and Qiantangjiang rivers in Group 2 lie south to the Changjiang River and share a similar nitrogen budget. The DIN and PON from Group 2 are mainly transported to the TUS and TAS sections. The Huaihe River (Group 4) is to the north of the Changjiang River and near the 34N section. Half of the input DIN from the Huaihe River is converted to PON, and nearly another half goes to the Yellow Sea through the 34N section, along with most generated PON in Group 4. The rivers of Groups 3 and 5 located outside of the ECS do not pump the nitrogen directly into the ECS but deliver it through the 34N section. After entering the ECS, the DINs from Groups 3 and 5 are assimilated or transported to the TUS section, the input and generated PON have two exits: the sediment and the TUS section. Among the riverine nitrogen budgets of the five groups, the total biological and physical fluxes of DIN_C (−1.84 and 1.93 kmol N s^{-1}) and PON_C (1.84 and −1.81 kmol N s^{-1}) account for approximately 90 % of those of all rivers (around 2.00 kmol N s^{-1}), indicating the dominant role of the Changjiang River in the riverine nitrogen budget.

3.4. DIN_C and PON_C budget comparison between the 1980s and 2010s

The nitrogen concentration in the Changjiang River water has dramatically increased since the 1970s (Liu et al., 2015). We designed a sensitivity experiment in which we changed only the DIN concentration in Changjiang River from 110.2 mmol m^{-3} to 33.5 mmol m^{-3}, which was an observed value in the 1980s (Zhang, 1996). Following this change, the annual Changjiang DIN_C loading flux reduced to 0.98 kmol s^{-1}. By comparing the DIN_C and PON_C budget in the 1980s and 2010s, we aim to recall the alterations in the nitrogen cycle and the corresponding environmental effect.

The input flux of DIN_C was three times larger in the 2010s than in the 1980s (Table 2). Compared to the 1980s, the generated PON_C in the 2010s increased by 219 %, 298 %, and 322 % over three shelf areas. The production efficiency of DIN_C in coastal areas was relatively low (Zhang et al., 2019a) because of the relatively low concentration of phosphorus. Increasing of nitrogen to phospate ratio in the Changjiang River has resulted in an unbalanced ratio between the nitrate concentration and phosphate in coastal water needed by the phytoplankton. The phosphorus deficiency occurred initially in the area directly impacted by the Changjiang River plume (Moon et al., 2020).

With less PON_C increase being generated, the export of the residual DIN_C by lateral transport notably increased by over 300 % across the 34N and TAS sections, and by more than 400 % across the TUS section, and 50-m, 100-m, and 200-m isobaths. The outflow of DIN_C and increase rate across the TUS section were the largest. As a result, more nutrients were transported to the continental shelf or open ocean instead of being converted to PON_C locally, thus increasing the environmental pressure there (Liu et al., 2019).

The increasing water–sediment flux rates of PON_C to the sea floor

Table 1
Annual mean of riverine DIN and PON budgets in the ECS. The Phy term is the sum of physical fluxes.

DIN budget	Group 1	Group 2	Group 3	Group 4	Group 5	Sum
(kmol N s^{-1})	Changjiang	Minjiang & Qiantangjiang	Rivers into the Bohai Sea	Huaihe	Yalujiang & Hanjiang	All rivers
Bio	−1.84	−1.09E-01	−3.50E-04	−2.64E-02	−2.25E-02	−2.00
Bot	5.71E-01	3.96E-02	1.14E-04	3.77E-03	9.87E-03	6.24E-01
200m	−3.39E-02	−1.15E-02	−2.28E-09	−6.80E-08	−1.14E-07	−4.53E-02
TUS	−9.98E-01	−5.56E-02	−2.40E-04	−2.30E-03	−1.41E-02	−1.07
34N	−4.58E-01	−5.84E-03	1.53E-03	−2.55E-02	3.88E-02	−4.49E-01
TAS	−3.67E-01	−7.54E-02	0.00	−3.97E-07	0.00	−4.42E-01
river	3.22	2.18E-01	0.00	5.25E-02	0.00	3.49
Phy	1.93	1.09E-01	1.40E-03	2.85E-02	3.46E-02	2.11
time-change	9.41E-02	3.31E-04	1.05E-03	2.13E-03	1.21E-02	1.10E-01
PON budget						
Bio	1.84	1.09E-01	3.50E-04	2.64E-02	2.25E-02	2.00
Bot	−1.26	−6.81E-02	−2.53E-04	−9.27E-03	−1.98E-02	−1.36
200m	−7.73E-03	−1.93E-03	−1.11E-09	−2.32E-08	−1.16E-07	−9.66E-03
TUS	−3.94E-01	−2.84E-02	−1.76E-04	−9.80E-04	−1.21E-02	−4.35E-01
34N	−8.92E-02	−1.37E-03	2.80E-04	−1.76E-02	1.21E-02	−9.58E-02
TAS	−5.64E-02	−1.56E-02	0.00	−8.12E-08	0.00	−7.20E-02
Phy	−1.81	−1.15E-01	−1.49E-04	−2.79E-02	−1.98E-02	−1.97
time-change	3.45E-02	−6.31E-03	2.01E-04	−1.46E-03	2.74E-03	2.96E-02

Table 2
Nitrogen budget comparison between the 2010s and 1980s. The DIN_C and PON_C fluxes lower than 1 are expressed in scientific notation. The values have units of kmol s^{-1}.

		2010s	1980s	2010s/1980s
River input		3.22	9.81E-01	328 %
	inner	1.27	5.81E-01	219 %
Bio	middle	2.83E-01	9.51E-02	298 %
	outer	2.91E-01	9.04E-02	322 %
DIN				
	inner	4.41E-01	2.11E-01	209 %
Bot	middle	8.73E-02	3.16E-02	276 %
	outer	4.25E-02	1.37E-02	310 %
200m		3.39E-02	7.76E-03	437 %
100m		1.29	3.00E-01	430 %
50m		1.85	4.54E-01	407 %
TUS		9.98E-01	2.14E-01	466 %
34N		4.58E-01	1.35E-01	339 %
TAS		3.67E-01	9.78E-02	375 %
PON				
	inner	1.05	4.79E-01	219 %
Bot	middle	1.31E-01	4.59E-02	285 %
	outer	7.93E-02	2.56E-02	310 %
200m		7.73E-03	2.19E-03	353 %
100m		1.88E-01	6.61E-02	284 %
50m		9.38E-02	3.89E-02	241 %
TUS		3.94E-01	1.27E-01	310 %
34N		8.92E-02	3.71E-02	240 %
TAS		5.64E-02	2.21E-02	255 %

were related to the generated PON_C over the three shelves. As the generated PON_C increased, the water–sediment fluxes of PON_C increased similarly by 219 %, 285 %, and 310 % over the three shelves. The increasing rates of lateral transports of PON_C were approximately 240 % at the 50-m isobath and 34N section while increasing substantially to over 300 % at the 200-m isobath and TUS section. The higher increases in lateral transports in the outer shelf correspond to the highest increase in generated PON_C.

3.5. New and export productions supported by DIN_C

Primary production can be divided into new production and regenerated production based on the nitrogen source (Dugdale and Goering, 1967). New production is related to nitrogen from outside the photic zone, which is also called the new nitrogen. Nitrogen from the rivers, atmospheric deposition, and open ocean are all external sources for new production over the ECS continental shelf. As discussed above, not all the DIN_C loading into the ECS can be assimilated due to limiting factors like phosphorus and light. An overestimation is inevitable if the new production in an area is based on the input flux of DIN_C (Chen et al., 1999).

Export production is the amount of carbon fixed by photic zone autotrophs, and either sinks to deeper water and sediments or is transported to open oceans. In a steady state, export production balances new production. In the open ocean, organic carbon exported below the seasonal thermocline is isolated from the upper ocean for over one hundred years. However, in the continental shelf, the carbon and nutrients regenerated below the euphotic layer can easily return to the euphotic layer and are reused by phytoplankton (Chen, 2003). Thus, the carbon export to sediment and open ocean rather than below the euphotic layer in the continental shelf plays an important role in long-term carbon sequestration (Simpson and Sharples, 2012; Stukel et al., 2015).

Considering the stable ratio of POC to PON (close to the Redfield ratio 6.63) in the ECS (Hung et al., 2000; Zhu et al., 2006), the export production due to DIN_C can be referred to as the sum of PON_C fluxes to open ocean and sediment. Treating the ECS shelf area as a whole, the exports of PON_C are water–sediment flux (0.69 kmol s^{-1}), lateral flux to the Japan Sea through the TUS section (0.39 kmol s^{-1}), lateral flux to the South China Sea through the TAS section (0.06 kmol s^{-1}), lateral flux across the 200-m isobath (0.01 kmol s^{-1}), and lateral flux to the Yellow Sea through the 34N section (0.09 kmol s^{-1}). Except for the last flux, they are all export production induced by the DIN_C in the ECS, adding up to 1.15 kmol N s^{-1}, among which the water–sediment flux and the export to the Japan Sea account for 60 % and 34 %, respectively.

In our model calculation, the gross primary production supported by DIN_C over the whole shelf is 12.71 kmol s^{-1}. The respiration of phytoplankton and remineralization of detritus are 7.42 and 3.45 kmol s^{-1}, respectively. Their sum (10.87 kmol s^{-1}) is the recycling flux of DIN_C, accounting for 85 % of the gross primary production. This percentage is similar to the estimation derived from the observation of the total nitrogen over the whole shelf (Zuo et al., 2016).

The ratio of export production to primary production (referred to as the e-ratio) related to the Changjiang River nitrogen is 0.09 (= 1.15/12.71), suggesting a handful of the primary production is exported. The e-ratio should be the same as the ratio of new production to primary production (referred to as the f-ratio). The f-ratio calculated from the relative concentration of nitrate is approximately 0.4 (Chen et al., 2001, 1999; Liu and Chai, 2009; Jiao et al., 1998). Hung et al. (2016) gave an e-ratio of 0.59 nearshore and 0.16 offshore based on trap-collected POC fluxes. Chen and Wang (1999) estimated an f-ratio of 0.15 based on the flux of new nutrients in a box model. Our e-ratio derived from DIN_C is

lower than the above studies for two reasons: the calculation method is different, and the DIN from the Changjiang River is not assimilated effectively, indicating a lower e-ratio than other external nitrogen sources.

As a carbon sink, the ECS absorbs approximately 6.92–23.30 Tg C yr^{-1} of atmospheric carbon dioxide (Jiao et al., 2018). The export production estimated here, 1.15 kmol N s^{-1}, is converted to POC fluxes of 2.89 Tg C yr^{-1}, accounting for 12–42 % of the carbon sequestration in the ECS. This percentage is comparable to an estimation of Chen (2000), 33 %).

4. Conclusions

Using the physical–biological coupled model and a tracking module, we examined the dissolved and particulate nitrogen budgets over the shelf area of the ECS, along with the roles of riverine nitrogen in export production. The horizontal distributions of DIN_C and PON_C generally follow the CDW and coastal currents and are affected by stratification in the vertical direction. The surface and bottom distributions of DIN_C are similar except for in summer, while the concentration of PON_C is larger in the bottom layer than in the surface layer year round.

The inventories of DIN_C and PON_C are affected by both biological and physical processes. Both of them changed dramatically in the inner shelf. Their time variations are dominated by biological fluxes and modulated by physical ones. The lateral transports of DIN_C are important exports in the DIN_C budget, among which that through the Tsushima Strait is the largest. With the increasing loading of DIN_C from the 1980s to the 2010s, the PON_C does not increase proportionally due to limited primary production. Consequently, residual DIN_C is transported further from the ECS, thereby increasing the environmental stress in the adjacent areas.

Most of the produced PON_C exports to the sediment, while some moves to the Tsushima Strait. According to the PON_C budget, its total export production is 1.15 kmol N s^{-1}, among which the flux to the sediment accounts for 60 % and the flux through the Tsushima Strait occupies 34 %. Based on the export production, it is estimated that DIN_C contributes approximately 12–42 % to the carbon sequestration of the ECS. The export production only occupies 0.09 of the total produced PON_C, suggesting a very low export efficiency.

Author statement

Jing Zhang: Software Visualization Writing - Original Draft. Xinyu Guo: Conceptualization Writing - Review & Editing. Liang Zhao: Methodology Writing - Review & Editing.

Declaration of competing interest

The authors declare that they have no known competing financial interests or personal relationships that could have appeared to influence the work reported in this paper.

Acknowledgments

We thank two anonymous reviewers for their valuable comments. This work was supported by the National Key Research and Development Program of China (2016YFC1401602), National Natural Science Foundation of China (42006018, 41876018), and Grants-in-Aid for Scientific Research (MEXT KAKENHI grant numbers: 20H04319). L. Zhao's participation of this study was supported by the Tianjin Natural Science Foundation (19JCZDJC40600). J. Zhang's participation of this study was supported by the Ministry of Education, Culture, Sports, Science and Technology, Japan (MEXT) under a Joint Usage/Research Center, Leading Academia in Marine and Environment Pollution Research (LaMer) Project and the Tianjin Municipal Education Commission Scientific Research Project (No. 2019KJ219).

References

Bi, R., Chen, X., Zhang, J., Ishizaka, J., Zhuang, Y., Jin, H., Zhang, H., Zhao, M., 2018. Water mass control on phytoplankton spatiotemporal variations in the northeastern east China Sea and the western Tsushima Strait revealed by lipid biomarkers. J. Geophys. Res. Biogeosciences 123, 1318–1332. https://doi.org/10.1002/2017JG004340.

Chang, P., Isobe, A., 2003. A numerical study on the Changjiang diluted water in the Yellow and East China Seas. J. Geophys. Res. 108, 3299. https://doi.org/10.1029/2002JC001749.

Chen, C.T.A., 2008. Distributions of nutrients in the East China Sea and the south China sea connection. J. Oceanogr. 64, 737–751. https://doi.org/10.1007/s10872-008-0062-9.

Chen, C.T.A., 2003. New vs. export production on the continental shelf. Deep. Res. Part II Top. Stud. Oceanogr. 50, 1327–1333. https://doi.org/10.1016/S0967-0645(03)00026-2.

Chen, C.T.A., 2000. The three gorges dam: reducing the upwelling and thus productivity in the East China sea. Geophys. Res. Lett. 27, 381–383. https://doi.org/10.1029/1999GL002373.

Chen, C.T.A., Wang, S.L., 1999. Carbon, alkalinity and nutrient budgets on the East China Sea continental shelf. J. Geophys. Res. Ocean. 104, 20675–20686. https://doi.org/10.1029/1999jc900055.

Chen, Y.L.L., Chen, H.Y., Lee, W.H., Hung, C.C., Wong, G.T.F., Kanda, J., 2001. New production in the East China Sea, comparison between well-mixed winter and stratified summer conditions. Continent. Shelf Res. 21, 751–764. https://doi.org/10.1016/S0278-4343(00)00108-4.

Chen, Y.L.L., Lu, H.B., Shiah, F.K., Gong, G.C., Liu, K.K., Kanda, J., Lee Chen, Y.L., Lu, H. B., Shiah, F.K., Gong, G.C., Liu, K.K., Kanda, J., Chen, Y.L.L., Lu, H.B., Shiah, F.K., Gong, G.C., Liu, K.K., Kanda, J., 1999. New production and F-ratio on the continental shelf of the East China Sea: comparisons between nitrate inputs from the subsurface Kuroshio current and the Changjiang river. Estuar. Coast Shelf Sci. 48, 59–75. https://doi.org/10.1006/ecss.1999.0404.

Dai, Z., Du, J., Zhang, X., Su, N., Li, J., 2011. Variation of riverine material loads and environmental consequences on the Changjiang (Yangtze) Estuary in recent decades (1955-2008). Environ. Sci. Technol. 45, 223–227. https://doi.org/10.1021/es103026a.

Dugdale, R.C., Goering, J.J., 1967. Uptake of new and regenerated forms of nitrogen in primary productivity. Limnol. Oceanogr. 12, 196–206. https://doi.org/10.4319/lo.1967.12.2.0196.

Estrada-Allis, S.N., Sheinbaum Pardo, J., Correia De Souza, J.M.A., Elizabeth Enríquez Ortiz, C., Mariño Tapia, I., Herrera-Silveira, J.A., 2020. Dissolved inorganic nitrogen and particulate organic nitrogen budget in the Yucatán shelf: driving mechanisms through a physical-biogeochemical coupled model. Biogeosciences 17, 1087–1111. https://doi.org/10.5194/bg-17-1087-2020.

Fennel, K., Wilkin, J., Levin, J., Moisan, J., O'Reilly, J., Haidvogel, D., 2006. Nitrogen cycling in the middle atlantic bight: results from a three-dimensional model and implications for the north atlantic nitrogen budget. Global Biogeochem. https://doi.org/10.1029/2005GB002456. Cycles 20.

Gao, X., Song, J., 2005. Phytoplankton distributions and their relationship with the environment in the Changjiang Estuary, China. Mar. Pollut. Bull. 50, 327–335. https://doi.org/10.1016/j.marpolbul.2004.11.004.

Große, F., Fennel, K., Zhang, H., Laurent, A., 2020. Quantifying the contributions of riverine vs. oceanic nitrogen to hypoxia in the East China Sea. Biogeosciences 17, 2701–2714. https://doi.org/10.5194/bg-17-2701-2020.

Guo, F., Li, Z., Shi, J., Qin, Y., 2015. Mutative trend of water quality at Xuliujing monitoring intersect on Yangtze river and the pollutants flux flowing into the sea during 2005–2012. Resour. Environ. Yangtze Basin 24, 227–232 (in Chinese).

Howarth, R.W., 2008. Coastal nitrogen pollution: a review of sources and trends globally and regionally. Harmful Algae 8, 14–20. https://doi.org/10.1016/j.hal.2008.08.015.

Hung, C.C., Chen, Y.F., Hsu, S.C., Wang, K., Chen, J.F., Burdige, D.J., 2016. Using rare earth elements to constrain particulate organic carbon flux in the East China Sea. Sci. Rep. 6, 33880. https://doi.org/10.1038/srep33880.

Hung, J.J., Lin, P.L., Liu, K.K., 2000. Dissolved and particulate organic carbon in the southern East China Sea. Continent. Shelf Res. 20, 545–569. https://doi.org/10.1016/S0278-4343(99)00085-0.

Isobe, A., Ando, M., Watanabe, T., Senjyu, T., Sugihara, S., Manda, A., 2002. Freshwater and temperature transports through the tsushima-korea straits. J. Geophys. Res. 107, 3065. https://doi.org/10.1029/2000JC000702.

Isobe, A., Matsuno, T., 2008. Long-distance nutrient-transport process in the Changjiang river plume on the East China Sea shelf in summer. J. Geophys. Res. Ocean. 113, C04006. https://doi.org/10.1029/2007JC004248.

Jiao, N., Liang, Y., Zhang, Yongyu, Liu, J., Zhang, Yao, Zhang, R., Zhao, M., Dai, M., Zhai, W., Gao, K., Song, J., Yuan, D., Li, C., Lin, G., Huang, X., Yan, H., Hu, L., Zhang, Z., Wang, L., Cao, C., Luo, Y., Luo, T., Wang, N., Dang, H., Wang, D., Zhang, S., 2018. Carbon pools and fluxes in the China Seas and adjacent oceans. Sci. China Earth Sci. https://doi.org/10.1007/s11430-018-9190-x.

Jiao, N.Z., Wang, R., Li, C.L., 1998. Primary production and new production in spring in the East China Sea. Oceanol. Limnol. Sinica 29, 135–140 (in Chinese).

Kawamiya, M., 2001. Mechanism of offshore nutrient supply in the western Arabian Sea. J. Mar. Res. 59, 675–696. https://doi.org/10.1357/002224001762674890.

Kwon, H.K., Kim, G., Hwang, J., Lim, W.A., Park, J.W., Kim, T.H., 2018. Significant and conservative long-range transport of dissolved organic nutrients in the Changjiang diluted water. Sci. Rep. 8, 1–7. https://doi.org/10.1038/s41598-018-31105-1.

Li, G., Han, X., Yue, S., Wen, G., Rongmin, Y., Kusky, T.M., 2006. Monthly variations of water masses in the East China Seas. Continent. Shelf Res. 26, 1954–1970. https://doi.org/10.1016/j.csr.2006.06.008.

Li, H.-M., Tang, H.-J., Shi, X.-Y., Zhang, C.-S., Wang, X.-L., 2014. Increased nutrient loads from the changjiang (yangtze) river have led to increased harmful algal blooms. Harmful Algae 39, 92–101. https://doi.org/10.1016/J.HAL.2014.07.002.

Liang, C., Xian, W., 2018. Changjiang nutrient distribution and transportation and their impacts on the estuary. Continent. Shelf Res. 165, 137–145. https://doi.org/10.1016/j.csr.2018.05.001.

Liu, G., Chai, F., 2009. Seasonal and interannual variability of primary and export production in the South China Sea: a three-dimensional physical-biogeochemical model study. ICES J. Mar. Sci. 66, 420–431. https://doi.org/10.1093/icesjms/fsn219.

Liu, K.-K., Yan, W., Lee, H.-J., Chao, S.-Y., Gong, G.-C., Yeh, T.-Y., 2015. Impacts of increasing dissolved inorganic nitrogen discharged from Changjiang on primary production and seafloor oxygen demand in the East China Sea from 1970 to 2002. J. Mar. Syst. 141, 200–217. https://doi.org/10.1016/j.jmarsys.2014.07.022.

Liu, S.M., Hong, G.H., Zhang, J., Ye, X.W., Jiang, X.L., 2009. Nutrient budgets for large Chinese estuaries. Biogeosciences 6, 2245–2263. https://doi.org/10.5194/bg-6-2245-2009.

Liu, S.M., Ning, X., Dong, S., Song, G., Wang, L., Altabet, M.A., Zhu, Z., Wu, Y., Ren, J.L., Liu, C.G., Zhang, J., Huang, D., 2020. Source versus recycling influences on the isotopic composition of nitrate and nitrite in the East China sea. J. Geophys. Res.: Oceans. https://doi.org/10.1029/2020JC016061.

Liu, X., Beusen, A.H.W., Van Beek, L.P.H., Mogollón, J.M., Ran, X., Bouwman, A.F., 2018. Exploring spatiotemporal changes of the Yangtze River (changjiang) nitrogen and phosphorus sources, retention and export to the East China Sea and Yellow Sea. Water Res. 142, 246–255. https://doi.org/10.1016/j.watres.2018.06.006.

Liu, Y., Deng, B., Du, J., Zhang, G., Hou, L., 2019. Nutrient burial and environmental changes in the Yangtze Delta in response to recent river basin human activities. Environ. Pollut. 249, 225–235. https://doi.org/10.1016/j.envpol.2019.03.030.

Lohrenz, S.E., Fahnenstiel, G.L., Redalje, D.G., Lang, G.A., Chen, X., Dagg, M.J., 1997. Variations in primary production of northern Gulf of Mexico continental shelf waters linked to nutrient inputs from the Mississippi river. Mar. Ecol. Prog. Ser. 155, 45–54. https://doi.org/10.3354/meps155045.

Ménesguen, A., Cugier, P., Leblond, I., 2006. A new numerical technique for tracking chemical species in a multi-source, coastal ecosystem, applied to nitrogen causing Ulva blooms in the Bay of Brest (France). Limnol. Oceanogr. 51, 591–601.

Moon, J.Y., Lee, K., Lim, W.A., Lee, E., Dai, M., Choi, Y.H., Han, I.S., Shin, K., Kim, J.M., Chae, J., 2020. Anthropogenic nitrogen is changing the East China and Yellow seas from being N deficient to being P deficient. Limnol. Oceanogr. 1–11 https://doi.org/10.1002/lno.11651.

Morimoto, A., Watanabe, A., Onitsuka, G., Takikawa, T., Moku, M., Yanagi, T., 2012. Interannual variations in material transport through the eastern channel of the Tsushima/Korea Straits. Prog. Oceanogr. 105, 38–46. https://doi.org/10.1016/j.pocean.2012.04.011.

Oey, L.-Y., Chang, Y.-L., Lin, Y.-C., Chang, M.-C., Varlamov, S., Miyazawa, Y., 2014. Cross flows in the Taiwan Strait in winter. J. Phys. Oceanogr. 44, 801–817. https://doi.org/10.1175/JPO-D-13-0128.1.

Quan, Q., Mao, X., Yang, X., Hu, Y., Zhang, H., Jiang, W., 2013. Seasonal variations of several main water masses in the southern Yellow Sea and East China Sea in 2011. J. Ocean Univ. China 12, 524–536. https://doi.org/10.1007/s11802-013-2198-5.

Shibano, R., Morimoto, A., Takayama, K., Takikawa, T., Ito, M., 2019. Response of lower trophic ecosystem in the Japan Sea to horizontal nutrient flux change through the Tsushima Strait. Estuar. Coast Shelf Sci. 229, 106386. https://doi.org/10.1016/j.ecss.2019.106386.

Simpson, J.H., Sharples, J., 2012. Introduction to the Physical and Biological Oceanography of Shelf Seas. Cambridge University Press.

Stukel, M.R., Benitez-Nelson, C.R., Decima, M., Taylor, A.G., Buchwald, C., Landry, M.R., 2015. The biological pump in the Costa Rica Dome: an open-ocean upwelling system with high new production and low export. J. Plankton Res. 38, 348–365. https://doi.org/10.1093/plankt/fbv097.

Umezawa, Y., Yamaguchi, A., Ishizaka, J., Hasegawa, T., Yoshimizu, C., Tayasu, I., Yoshimura, H., Morii, Y., Aoshima, T., Yamawaki, N., 2014. Seasonal shifts in the contributions of the changjiang river and the kuroshio current to nitrate dynamics in the continental shelf of the northern east China sea based on a nitrate dual isotopic composition approach. Biogeosciences 11, 1297–1317. https://doi.org/10.5194/bg-11-1297-2014.

Wang, B., 2006. Cultural eutrophication in the changjiang (Yangtze River) plume: history and perspective. Estuar. Coast Shelf Sci. 69, 471–477. https://doi.org/10.1016/J.ECSS.2006.05.010.

Wang, W., Yu, Z., Song, X., Wu, Z., Yuan, Y., Zhou, P., Cao, X., 2017. Characteristics of the δ 15 N NO 3 distribution and its drivers in the Changjiang River estuary and adjacent waters. Chin. J. Oceanol. Limnol. 35, 367–382. https://doi.org/10.1007/s00343-016-5276-x.

Wang, Y., Guo, X., Zhao, L., Zhang, J., 2019. Seasonal variations in nutrients and biogenic particles in the upper and lower layers of East China Sea Shelf and their export to adjacent seas. Prog. Oceanogr. 176, 102138. https://doi.org/10.1016/j.pocean.2019.102138.

Wu, H., Deng, B., Yuan, R., Hu, J., Gu, J., Shen, F., Zhu, J., Zhang, J., 2013. Detiding measurement on transport of the Changjiang-derived buoyant coastal current. J. Phys. Oceanogr. 43, 2388–2399. https://doi.org/10.1175/JPO-D-12-0158.1.

Xue, Z., He, R., Fennel, K., Cai, W.-J., Lohrenz, S., Hopkinson, C., 2013. Modeling ocean circulation and biogeochemical variability in the Gulf of Mexico. Biogeosciences 10.

Yan, X., Xu, M.N., Wan, X.S., Yang, J.-Y.T.Y.T., Trull, T.W., Dai, M., Kao, S.-J.J., 2017. Dual isotope measurements reveal zoning of nitrate processing in the summer changjiang (yangtze) River plume. Geophys. Res. Lett. 44, 12,289–12,297. https://doi.org/10.1002/2017GL075951.

Yu, Y., Song, J., Li, X., Yuan, H., Li, N., 2012. Distribution, sources and budgets of particulate phosphorus and nitrogen in the East China Sea. Continent. Shelf Res. 43, 142–155. https://doi.org/10.1016/j.csr.2012.05.018.

Zhang, J., 1996. Nutrient elements in large Chinese estuaries. Continent. Shelf Res. 16, 1023–1045. https://doi.org/10.1016/0278-4343(95)00055-0.

Zhang, J., Guo, X., Zhao, L., 2019a. Tracing external sources of nutrients in the East China Sea and evaluating their contributions to primary production. Prog. Oceanogr. 176, 102122. https://doi.org/10.1016/j.pocean.2019.102122.

Zhang, J., Guo, X., Zhao, L., Miyazawa, Y., Sun, Q., 2017. Water exchange across isobaths over the continental shelf of the East China sea. J. Phys. Oceanogr. 47, 1043–1060. https://doi.org/10.1175/JPO-D-16-0231.1.

Zhang, J., Liu, S.M., Ren, J.L., Wu, Y., Zhang, G.L., 2007. Nutrient gradients from the eutrophic changjiang (Yangtze River) estuary to the oligotrophic kuroshio waters and re-evaluation of budgets for the East China sea shelf. Prog. Oceanogr. 74, 449–478. https://doi.org/10.1016/j.pocean.2007.04.019.

Zhang, S., Ji, H., Yan, W., Duan, S., 2003. Composition and flux of nutrients transport to the Changjiang Estuary. J. Geogr. Sci. 13, 3–12. https://doi.org/10.1007/bf02873141.

Zhang, S., Stock, C.A., Curchitser, E.N., Dussin, R., 2019b. A numerical model analysis of the mean and seasonal nitrogen budget on the northeast U.S. Shelf. J. Geophys. Res. Ocean. 124, 2969–2991. https://doi.org/10.1029/2018JC014308.

Zhao, L., Guo, X., 2011. Influence of cross-shelf water transport on nutrients and phytoplankton in the East China Sea: a model study. Ocean Sci. 7, 27–43. https://doi.org/10.5194/os-7-27-2011.

Zhong, X., Yan, M., Ning, X., Yan, Z., Xin, Y., 2020. Nitrate processing traced by nitrate dual isotopic composition in the early spring in the Changjiang (Yangtze River) Estuary and adjacent shelf areas. Mar. Pollut. Bull. 161, 111699. https://doi.org/10.1016/j.marpolbul.2020.111699.

Zhu, Z.Y., Zhang, J., Wu, Y., Lin, J., 2006. Bulk particulate organic carbon in the East China Sea: tidal influence and bottom transport. Prog. Oceanogr. 69, 37–60. https://doi.org/10.1016/j.pocean.2006.02.014.

Zuo, J., Song, J., Yuan, H., Li, X., Li, N., Duan, L., 2016. Particulate nitrogen and phosphorus in the East China Sea and its adjacent kuroshio waters and evaluation of budgets for the East China sea shelf. Continent. Shelf Res. 131, 1–11. https://doi.org/10.1016/j.csr.2016.11.003.